AD-A087 747 ROME AIR DEVELOPMENT CENTER GRIFFISS AFB NY F/G 20/14
MULTIPATH PROPAGATION OVER SNOW AT MILLIMETER WAVELENGTHS,(U)
FEB 80 U H LAMMERS, D T HAYES
UNCLASSIFIED RADC-TR-80-54 NL

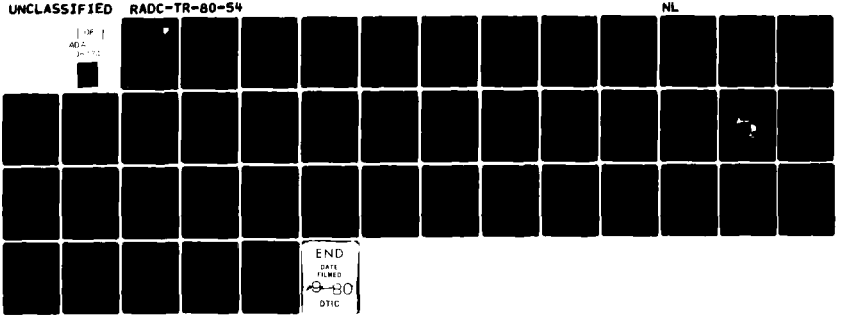

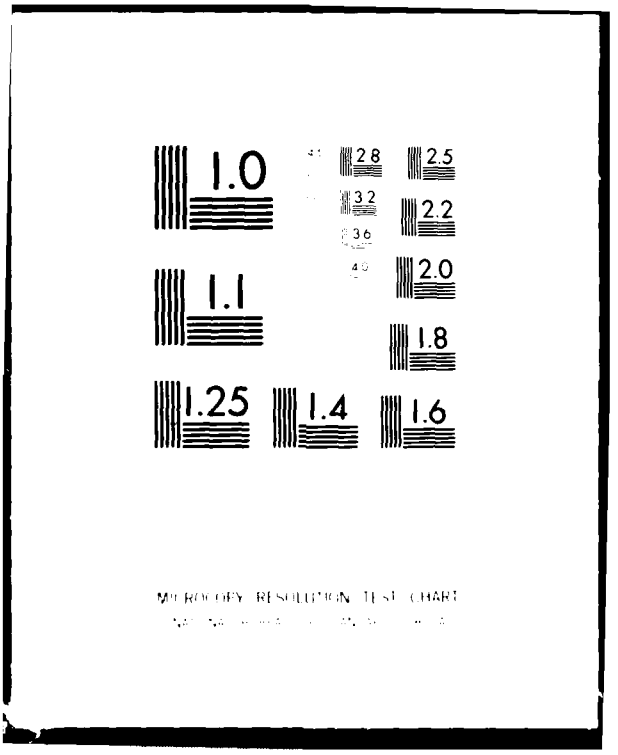
1.0
2.8
2.5
3.2
2.2
3.6
4.0
2.0
1.1
1.8
1.25
1.4
1.6
MICROCOPY RESOLUTION TEST CHART

RADC-TR-80-54
In-House Report
February 1980

MULTIPATH PROPAGATION OVER SNOW AT MILLIMETER WAVELENGTHS

Uve H.W. Lammers
Dallas T. Hayes

ROME AIR DEVELOPMENT CENTER
Air Force Systems Command
Griffiss Air Force Base, New York 13441

This report has been reviewed by the RADC Public Affairs Office (PA) and is releasable to the National Technical Information Service (NTIS). At NTIS it will be releasable to the general public, including foreign nations.

RADC-TR-80-54 has been reviewed and is approved for publication.

APPROVED: Edward A. Lewis
EDWARD A. LEWIS
Chief, Propagation Branch
Electromagnetic Sciences Division

APPROVED: Allan C. Schell
ALLAN C. SCHELL, Chief
Electromagnetic Sciences Division

FOR THE COMMANDER: John P. Huss
JOHN P. HUSS
Acting Chief, Plans Office

If your address has changed or if you wish to be removed from the RADC mailing list, or if the addressee is no longer employed by your organization, please notify RADC (EEP), Hanscom AFB MA 01731. This will assist us in maintaining a current mailing list.

Do not return this copy. Retain or destroy.

Unclassified

SECURITY CLASSIFICATION OF THIS PAGE (When Data Entered)

REPORT DOCUMENTATION PAGE	READ INSTRUCTIONS BEFORE COMPLETING FORM
1. REPORT NUMBER: RADC-TR-80-54 ✓ 2. GOVT ACCESSION NO: AD-A087 747	3. RECIPIENT'S CATALOG NUMBER
4. TITLE (and Subtitle): MULTIPATH PROPAGATION OVER SNOW AT MILLIMETER WAVELENGTHS	5. TYPE OF REPORT & PERIOD COVERED: In-house
	6. PERFORMING ORG. REPORT NUMBER
7. AUTHOR(s): Uve H.W. Lammers, Dallas T. Hayes	8. CONTRACT OR GRANT NUMBER(s)
9. PERFORMING ORGANIZATION NAME AND ADDRESS: Deputy for Electronic Technology (RADC/EEP) Hanscom AFB Massachusetts 01731	10. PROGRAM ELEMENT, PROJECT, TASK AREA & WORK UNIT NUMBERS: 46001607
11. CONTROLLING OFFICE NAME AND ADDRESS: Deputy for Electronic Technology (RADC/EEP) Hanscom AFB Massachusetts 01731	12. REPORT DATE: February 1980
	13. NUMBER OF PAGES: 44
14. MONITORING AGENCY NAME & ADDRESS(if different from Controlling Office)	15. SECURITY CLASS. (of this report): Unclassified
	15a. DECLASSIFICATION DOWNGRADING SCHEDULE

16. DISTRIBUTION STATEMENT (of this Report)

Approved for public release; distribution unlimited.

17. DISTRIBUTION STATEMENT (of the abstract entered in Block 20, if different from Report)

18. SUPPLEMENTARY NOTES

19. KEY WORDS (Continue on reverse side if necessary and identify by block number)

Millimeter-wave propagation
Multipath propagation
Snow cover
Terrain scatter

20. ABSTRACT (Continue on reverse side if necessary and identify by block number)

A series of multipath measurements over snow were conducted at Hanscom AFB during the winter 1978/79. Data were obtained over a path-length of 179.5 m at frequencies of 35, 98, and 140 GHz. The gently rolling grass-covered terrain showed maximum height differences of 0.8 m. Snow covers included freshly fallen snow, old metamorphic snow, and sleet. The equipment consisted of CW transmitters at 2-m height and receivers mounted on a vertical positioner to measure the height-gain pattern of the received signal between 0.2- and 4-m height. Grazing angles for this geometry range

DD FORM 1 JAN 73 1473

Unclassified

SECURITY CLASSIFICATION OF THIS PAGE (When Data Entered)

20. (Cont)

between 0.5 and 2 degrees. Measured interference patterns between direct and terrain-reflected rays were generally coherent in appearance and exhibited cancellation depths to 20 dB and lower, depending on the type of snow cover. A computer program was developed in order to model the reflection as a specular process, with the underlying terrain represented by a series of linear sloping segments, derived from actual terrain height measurements. With appropriate transitions between the linear segments and reflection coefficients calculated from relevant snow parameters, calculated and measured height-gain patterns display quite similar qualities.

Preface

The authors would like to acknowledge the contributions of several members of the Propagation Branch to this project. Mr. J. T. Doherty participated in the measurements and did the computer programming. Mr. R. A. Marr built the specialized digital data recording system. Capt. J. J. McNally helped with the measurements and the processing and plotting of the experimental data.

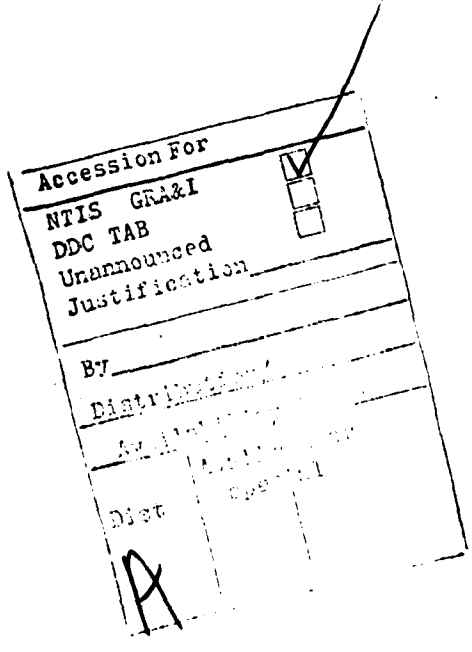

Contents

Illustrations

Tables

Multipath Propagation Over Snow at Millimeter Wavelengths

1. INTRODUCTION

During the winter of 1977/78 RADC conducted a measurement program on the backscatter properties of metamorphic snow. In the completely frozen state this type of ground cover exhibits strong reflective properties at millimeter wavelengths. Depending on the frequency and the grazing angle at which a radar beam intercepts the surface, the amount of backscatter may be substantially decreased when the snow begins to melt. Results from these measurements are incorporated in an RADC Technical Report.[1]

Snow backscatter is not the only terrain interaction of concern. Typical near-surface systems, both radar and line-of-sight, have to contend with multipath propagation due to diffuse forward scatter or specular reflection from a snow layer on the ground. It is necessary to determine the type and severity of this interference mechanism in order to complement the backscatter data previously obtained.

Equipment used in the backscatter measurements was modified in such a way that transmitters and receivers could be operated in separate locations. The measurements were made at the same frequencies (35, 98, and 140 GHz) as in the

(Received for publication 21 February 1980)

1. Hayes, D.T., Lammers, U.H.W., and Marr, R.A. (1980) Scattering From Snow Backgrounds at 35, 98, and 140 GHz, RADC Tech Rep. (to be published).

backscatter experiment. The equipment transmits CW signals and uses antenna beams of sufficient width to encompass both direct and reflected signals. Three methods are available for separating the components of a received signal for measurement: (a) time-of-arrival difference, (b) angle-of-arrival difference, and (c) phase interference pattern. Method (c) was used since the equipment does not provide temporal or adequate angular resolution.

The inherent weather-dependent attenuation restricts millimeter-wave systems operating near the earth surface to ranges of a few kilometers. On tactical ground-to-ground paths one assumes antenna heights on the order of two meters. This results in grazing angles on snow of less than one degree. On air-to-ground and ground-to-air paths one of the terminals will be at greater height, alleviating the multipath problem to some extent. However, grazing angles of a few degrees under most weather conditions and sufficiently long range are possible.

Limitations of the existing equipment restrict the transmitter/receiver distance in snow multipath measurements to several hundred meters, if sufficient dynamic range for the determination of constructive and destructive multipath interference is to be maintained. Transmitter and receiver heights are easily scaled to cover a realistic range of grazing angles. The range limitation has a side benefit. Better uniformity of the terrain and snow cover is likely because of a smaller antenna footprint area.

Multipath measurements over snow were performed during the winter 1978/79. Because of abnormal weather patterns, very few significant snowfalls occurred during that season in the Boston area, never leaving an extensive snow layer on the ground for a long time period. For this reason only a limited number of measurements were obtained. Typical melt/freeze cycles, as they had been experienced during the previous winters, did not occur. Despite the shortcomings of the weather, substantial multipath effects were observed at all frequencies. The unavailability in the literature of snow multipath data at millimeter wavelengths and the current widespread interest in this type of information suggested a publication of these preliminary results.

2. ANALYSIS OF MULTIPATH PROPAGATION

A phase interference pattern is established by the direct and reflected waves from a transmitter operating near terrain. Probing of the interference pattern provides a simple method to separate the wave components and to determine the reflective properties of the terrain. In Figure 1 a schematic view is presented of the experimental system used, with the transmitting antenna mounted at a fixed height h_T above ground and the receiving antenna, at distance r_{TR}, moving

perpendicularly to the ground over a height range approximately equal to h_R. Vertical motion of the receiving antenna results in an almost maximum rate of change of path difference between the direct and reflected waves. For a given height range over which the receiving antenna travels, this yields a maximum number of 2π-phase revolutions for any given wavelength. Over flat terrain the point of specular reflection travels in the direction from the transmitter to the receiver as the receiver antenna moves from h_{Rmax} to h_{Rmin}. The minimum displacement of the reflection point on the ground necessary in probing received signal levels at adjacent points of most constructive and destructive phase interference is also achieved when the probe travels vertically. In order to measure multipath reflection centered at a fixed point on the ground with the phase interference method, one could change transmitter and receiver height simultaneously. This was considered a complication of the experimental procedure, not worth the advantage gained. A need exists anyhow, to conduct measurements over a large number of surfaces to average out local effects and to establish the range of multipath signal levels resulting from local peculiarities. The influence of the surface area over which reflection takes place may be studied separately by moving the probe parallel to the ground at a fixed height h_R. In this case all parameters except for the reflection area are constant when the probe moves along a circular path around the transmitter.

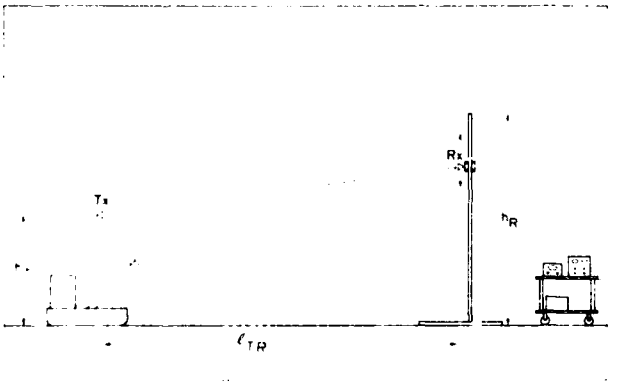

Figure 1. Schematic View of Experimental Multipath Measurement System

2.1 Propagation Mechanisms

In conducting low-angle bistatic propagation measurements over snow, we have to consider a series of parameters that affect the scatter or reflection process. Snow is an ice-air or ice-water-air mixture, whose dielectric properties range between those of air (lossless), ice (low loss), and water (high loss) at millimeter wavelengths. In the freshly fallen fluffy state, snow constitutes a fairly uniform mixture of air and ice. In a late metamorphic state, it contains distinct spherical structures of ice or water-coated ice, several millimeters in diameter, sometimes with a thin ice layer on top. Attenuation in snow increases with frequency. As a surface, snow follows the local terrain contour in places, it smooths it out in others, or produces its own windblown surface structure.

Three distinct processes are conceivable to produce multipath signals over snow-covered terrain: (a) diffuse or specular surface scatter from snow, (b) incoherent volume scatter from snow, and (c) diffuse or specular surface scatter from the underlying terrain. Whether or not (b) and (c) produce significant contributions to the received signal depends on factors like the snow depth, the type of snow, the grazing angle, and frequency. At the low grazing angles under consideration, the total pathlength that a terrain-reflected signal travels through snow is substantial. At a snow depth of 0.1 m, for example, grazing angles of 0.1, 1, and 10 deg lead to snow paths of 115, 11.5, and 1.2 m, respectively. Attenuation through slabs of dry metamorphic snow, approximately 0.1 m thick, was measured[1] at 35 GHz (12 dB/m), 98 GHz (150 dB/m), and 140 GHz (200 dB/m). These numbers demonstrate that for most grazing angles and frequencies the contribution from the underlying terrain must be insignificant. Water in the snow further increases attenuation. To a degree the same argument applies to volume scatter from within the snow layer. With the exception of scatterers close to the surface, signals are strongly attenuated. As will be shown, actual snow multipath data at millimeter wavelengths appear to be highly coherent in contrast to backscatter data taken with the same equipment over similar snow. This further supports the assumption that volume scatter from within the snow layer does not contribute significantly to the terrain-returned component of the received signal. Based on experimental results obtained to date, we assume that multipath returns from snow can be modeled as a surface or near-surface effect, with the pathlength differences between individual scatterers or the surface roughness small enough in terms of the Rayleigh criterion to produce a coherent signal.

2.2 Model Calculations for Flat Terrain

In order to study the effects that simplifying assumptions like the negligible dependence on the beam pattern have on signal cancellation depth, an analytical

model was designed. The model describes snow multipath propagation at millimeter wavelengths by specular reflection from a surface profile composed of linear and circular sections to fit the actual profile over which the measurements were made. Consider Figure 2, in which a six-segment linear profile is indicated, defined by segment heights h_0 through h_6 and segment lengths ℓ_1 through ℓ_6. The transmitter antenna, located at $\ell = 0$ and height $h_0 + h_T$, radiates with a Gaussian beam pattern

$$G_T = e^{-A(\beta_{TR} - \delta)^2}, \tag{1}$$

where A is a multiplier depending on the antenna 3 dB-beamwidth, β_{TR} is the angle between the ray to be reflected and the horizontal direction, and δ is the angle at which the beam is tilted against the horizontal direction. Similarly, the receiving antenna beam is defined as

$$G_R = e^{-A(\beta_{RR} - \delta)^2}. \tag{2}$$

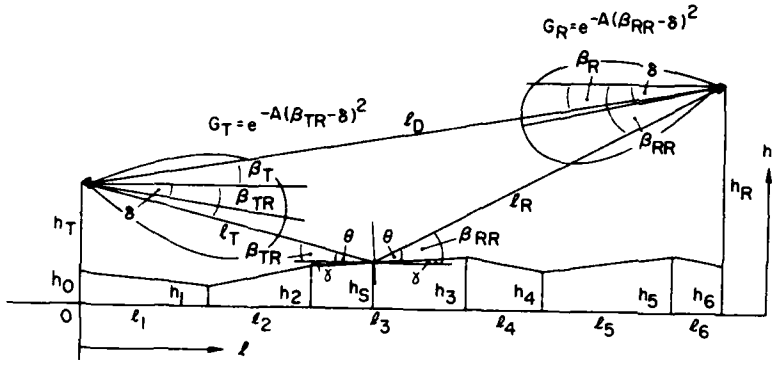

Figure 2. Specular Multipath Propagation Model (Six-Segment Linear Terrain Profile)

Assume now that a ray from the transmitter, ℓ_T, is impinging at point S, which is at height h_S above the reference level

$$h_S = h_{n-1} + (\ell - \sum_{1}^{m=n-1} \ell_m)(h_n - h_{n-1})/\ell_n . \tag{3}$$

Here n is the segment number in which h_S lies, ℓ is the distance from the transmitter to the reflection point, h_{n-1} and h_n are the heights at the left and right ends of the segment, ℓ_n is the segment length, and $\sum_{1}^{m=n-1} \ell_m$ is the sum of the segment lengths counting from $\ell = 0$ and including the one to the left of the segment in which h_S lies. The slope from which reflection takes place has the angle

$$\gamma = \tan^{-1}\left[(h_n - h_{n-1})/\ell_n\right] \tag{4}$$

with the horizontal direction. With θ the grazing angle and reflected angle on the local slope, we can write

$$\beta_{TR} + \gamma = \theta = \beta_{RR} - \gamma \tag{5}$$

and

$$\beta_{RR} = 2\gamma + \beta_{TR} .$$

With the angles known, the distance $\ell_T + \ell_R$ can be found that the reflected ray travels from the transmitter to the receiver

$$\ell_T = (\ell^2 + (h_T + h_o - h_S)^2)^{1/2} \tag{6}$$

$$\ell_R = [(\ell_{TR} - \ell)^2 + (h - h_S)^2]^{1/2} . \tag{7}$$

The term ℓ_{TR} denotes the transmitter-receiver horizontal distance. The reflected ray ℓ_R reaches the receiver ordinate at height h, where

$$h = h_S + (\ell_{TR} - \ell) \tan (\beta_{TR} + 2\gamma) . \tag{8}$$

Well below the Brewster angle, a phase shift approaching 180 deg is introduced upon reflection for both horizontal and vertical polarization. This is the case for the angles of interest here. The phase shift can be expressed as an additional path-length traveled by the reflected ray

$$s = \lambda/2 , \tag{9}$$

where λ is the wavelength.

The direct ray from the transmitter to the receiver traverses a distance

$$\ell_D = (\ell_{TR}^2 + (h - h_T - h_o)^2)^{1/2} . \tag{10}$$

The antenna gains in the direction of the direct ray are

$$G_T = e^{-A(\beta_T - \delta)^2} \tag{11}$$

$$G_R = e^{-A(\beta_R - \delta)^2} .$$

The computational procedure chosen moves the reflection point on the surface in increments of $\Delta\ell$ from $\ell = 0$ to ℓ_{TR}. The height h at which the reflected ray from each reflection point crosses the receiver ordinate is determined according to the local height and slope at that reflection point. If height h falls within the range h_R over which the probing receiver travels, a phasor addition is performed between the direct signal calculated for the same height h and the reflected signal. Depending on the distance of the reflection point from the transmitter and the local height and slope, multiple reflected signals may superimpose with the direct signal to form the sum signal at any particular height h. It is obvious that the simple terrain model drawn in Figure 2 results in discontinuities in the local slope when the reflection point transitions from one segment to the next. In this case the reflected signal breaks off at one height h and jumps to another one. In order to make the profile more realistic, circular transition regions between segments were introduced. These transition regions make the reflected signal vary continuously with height. The circular region is tangent to the present- and next-segment straight slopes. The circle diameter is determined by selecting a distance q between the present-segment tangent point and the end of that segment. In Figure 3 one such circular transition region is drawn between segments n and n+1. The slopes of these two segments are

$$\gamma_1 = \tan^{-1}\left[(h_n - h_{n-1})/\ell_n\right]$$

and

$$\gamma_2 = \tan^{-1}\left[(h_{n+1} - h_n)/\ell_{n+1}\right] . \tag{12}$$

Next the tangent points of the circle can be calculated

$$\begin{aligned} x_1 &= \ell_n - q \\ y_1 &= h_{n-1} + (\ell_n - q)\tan\gamma_1 \\ x_2 &= \ell_n + (q^2 - (y_1 - h_n)^2)^{1/2}\cos\gamma_2 \\ y_2 &= h_n + (q^2 - (y_1 - h_n)^2)^{1/2}\sin\gamma_2 . \end{aligned} \tag{13}$$

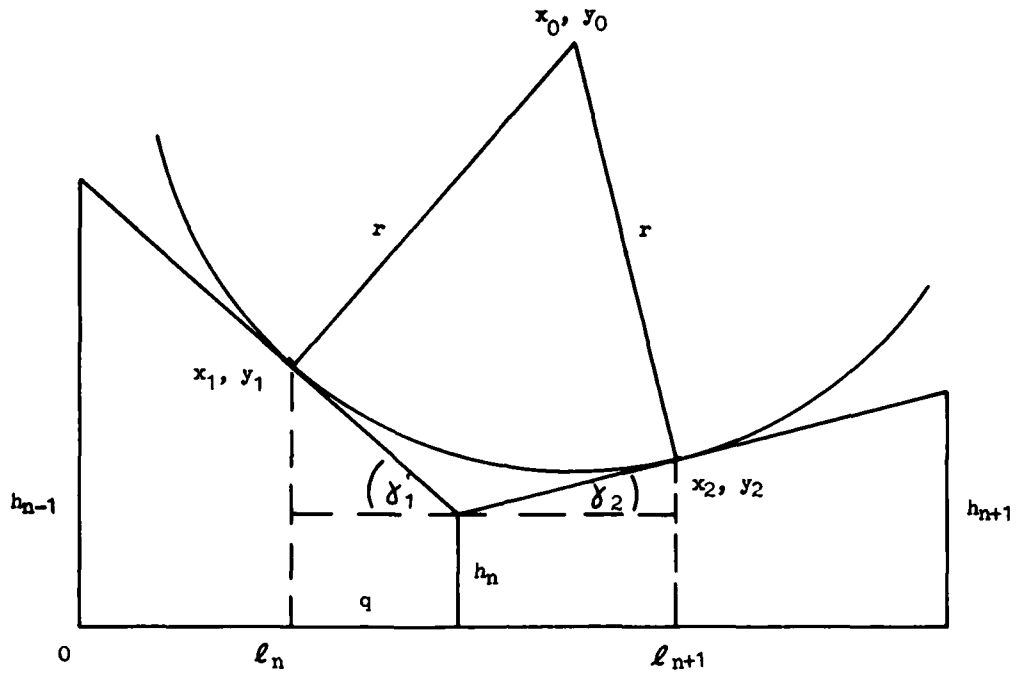

Figure 3. Geometry of Circular Segment Transition

The center coordinates of the circle are

$$x_o = (x_2 - x_1 \tan \gamma_2/\tan \gamma_1 + (y_2 - y_1) \tan \gamma_2)/(1 - \tan \gamma_2/\tan \gamma_1) \qquad (14)$$

and

$$y_0 = y_1 + (x_1 - x_0) \tan \gamma_1 .$$

Note, x_0, x_1, and x_2 are referenced to the left side of the present segment. The radius of the circle is

$$r = [(x_0 - x_1)^2 + (y_0 - y_1)^2]^{1/2} . \qquad (15)$$

The height of the reflection point in the circular region then becomes

$$h_S = (r^2 - (x - x_0)^2)^{1/2} + y_0 \qquad (16)$$

and the surface slope

$$\gamma = \tan^{-1}(-1/([r/(x - x_0)]^2 - 1)^{1/2}) . \quad (17)$$

For all receiver heights we assume that unity-magnitude signals are received independent of range and whether they propagate on a direct or indirect path. The sum signal then becomes

$$V = |G_T G_R e^{-j 2\pi \ell_D/\lambda} + G_T G_R \rho e^{-j 2\pi (\ell_T + \ell_R + s)/\lambda}| . \quad (18)$$

Note that G_T and G_R have to be taken along the directions of the particular rays. The magnitude of the reflection coefficient is ρ.

Barton[2] gives magnitudes of the reflection coefficient at grazing angles θ neglecting the small loss tangent of ice. For vertical polarization

$$\rho_V = (\epsilon_r \sin\theta - (\epsilon_r - \cos^2\theta)^{1/2})/(\epsilon_r \sin\theta + (\epsilon_r - \cos^2\theta)^{1/2})$$

and horizontal polarization

$$\rho_H = (\sin\theta - (\epsilon_r - \cos^2\theta)^{1/2}/(\sin\theta + (\epsilon_r - \cos^2\theta)^{1/2}) . \quad (19)$$

Barton references work of Cumming[3] who confirmed a theoretical expression for the dielectric constant ϵ_r of an air-ice mixture

$$(\epsilon_r - 1)/\epsilon_r = 3f(\epsilon_i - 1)/(\epsilon_i + 2\epsilon_r) . \quad (20)$$

Here f is the fractional volume occupied by solid ice and ϵ_i its dielectric constant. Complex refractive indices of ice and water at the experimental wavelength and 0 deg C are listed in Table 1, as taken from a survey by Ray.[4]

---

2. Barton, D.K. (1977) Reflection coefficients of snow, Appendix III in Multipath Measurements Phase III, Final Tech Rep. ER 77-4121, ARPA Order No. 2731.

3. Cumming, W.A. (1952) The dielectric properties of ice and snow at 3.2 centimeters, J. Appl. Phys. 23(No. 7):768-773.

4. Ray, P.S. (1972) Broadband complex refractive indices of ice and water, Appl. Optics 11(No. 8):1836-1844.

Table 1. Complex Refractive Indices of Ice and Water at 0 deg C

Wavelength (mm)	Ice		Water	
	n_r	n_i	n_r	n_i
8.6	1.78	9×10^{-4}	4.2	2.5
3.0	1.78	5×10^{-4}	2.7	1.3
2.1	1.78	3×10^{-4}	2.6	0.9

If we neglect the imaginary part n_i of the complex refractive index of ice, then its dielectric constant $\epsilon_i = n_r^2 = 3.15$ is constant over the wavelength range from 8.6 to 2.1 millimeters. Substituting for ϵ_i and solving for ϵ_r we obtain from Eq. (20)

$$\epsilon_r = 1.6125 f - 0.2875 + (1.575 + (1.6125 f - 0.2875)^2)^{1/2} . \quad (21)$$

If we assume that the path geometry makes it possible to neglect the effect of pathlength differences and antenna gain patterns on the signals received via direct and reflected paths, then a maximum signal of $1+\rho$ and a minimum signal of $1-\rho$ are received. This is based on a single reflected signal. The voltage ratio between adjacent maxima and minima becomes

$$\Delta V = 20 \log [(1 + \rho)/(1 - \rho)] \quad (22)$$

in decibel.

With close enough spacing between adjacent maxima and minima, so that changes in the measurement geometry and the snow surface are negligible, the reflection coefficient can be derived from the voltage ratio by reversing Eq. (22)

$$\rho = (10^{\Delta V/20} - 1)/(10^{\Delta V/20} + 1) . \quad (23)$$

If more than one reflected signal contributes to the received signal it becomes increasingly more difficult to separate individual contributions and to extract ρ.

A series of multipath signal calculations were performed based on these equations with flat terrain of zero height between transmitter and receiver. This simplification results in the superposition of the direct ray and only one reflected rav. Better insight into the effect of various system parameters is gained, when multiple reflected signals do not complicate the signal structure. Figure 4 shows the height-gain pattern of the received signal vs receiver height, for typical

parameters of the experimental system. At 35.1 GHz and vertical polarization a relative dielectric constant of 1.92 was chosen, corresponding to metamorphic snow. The antenna 3 dB-beamwidth of both transmitter and receiver antennas is 7 degrees. The beams are not tilted in elevation. For a pathlength ℓ_{TR} = 179.5 m, 10 maxima and minima are plotted as the receiver descends from 4 m to 0.2 m height. The transmitter is at a fixed height of 2 m. In Figure 4, 0 dB corresponds to the magnitude of the direct signal. In-phase superposition of a single reflected signal leads to a sum signal 6 dB higher. The sum signal level is essentially constant for all peaks, indicating that the multiplication by the antenna gain factors has little effect there. The more obvious influence can be seen in the minima, where a relatively minor change in the direct or reflected signal amplitude can make a substantial change in the signal cancellation. This is apparent as the receiving antenna moves from h_{Rmax}, where the reflected signal is at a disadvantage relative to the direct signal both in terms of antenna gain and reflection loss to h_{Rmin}, where the reflection loss disadvantage is compensated for by a somewhat higher antenna gain. Both signals are more closely matched, leading to a cancellation of up to 20 dB. Slight irregularities in the null depths are due to the finite length of the $\Delta\ell$ increment. The spacing between minima is practically constant over the height range. In Figure 5 the same curve is shown for a dielectric constant ϵ_r = 1.12, which is representative of very light and fluffy snow. Close inspection reveals a reduction of the maxima by approximately 0.3 dB and of the minima by approximately 2 dB. There is no lateral displacement of the curves. The next change in Figure 6 is to horizontal polarization. Its only effect is an increase in null depths by 0.5 dB, a result to be expected in view of the small differences between ρ_V and ρ_H as calculated from Eq. (19). Comparing Figures 6 and 7, we evaluate the effect that the width of the beams has on the multipath signal. Note again that the beamwidth was not chosen to discriminate against the terrain-reflected signal, as would be the case in most system applications. Instead, the idea is to employ a wide enough beam in order not to reduce the reflected ray. In the situation where the transmitting antenna is at h_T = 2 m, the receiving antenna is at h_R = 4 m, and the distance between them is ℓ_{TR} = 179.5 m, the largest angle is subtended between the direct and reflected rays. At the transmitter antenna this angle is 2.55 deg, which is a substantial fraction of the 3 dB-beamwidth of 7 degrees. Figure 7 is computed with a beamwidth of 35 deg, all other parameters being identical with Figure 6. We see that the greatest difference between the two curves indeed occurs near maximum receiver height. There is a slight shift of maxima and minima to lower height, a 1 dB-increase of the maxima and a 5 dB-decrease of the minima. These effects taper off to 0.3 dB and 1 dB respectively, as the receiver is lowered, with almost no height displacement between extremes.

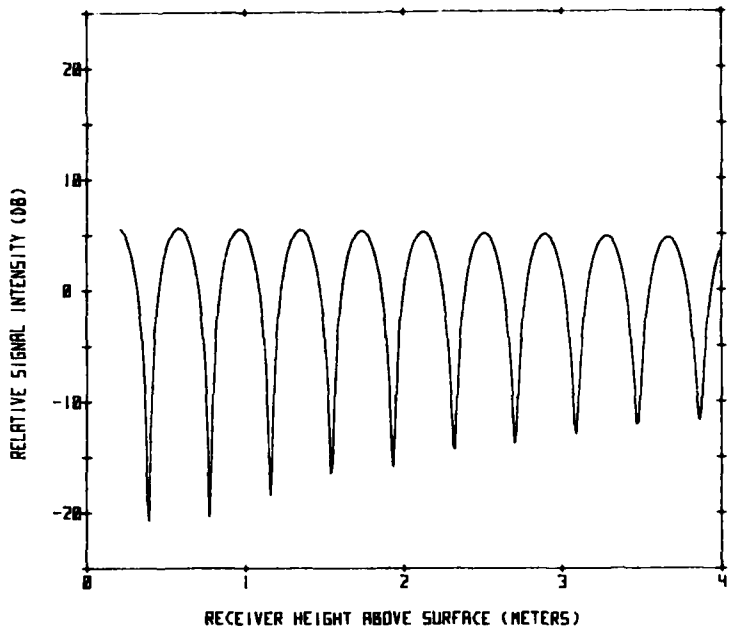

Figure 4. Multipath Signal Over Flat Surface (Frequency 35.1 GHz, Vertical Polarization, $\epsilon_r = 1.92$, Beamwidth 7 deg)

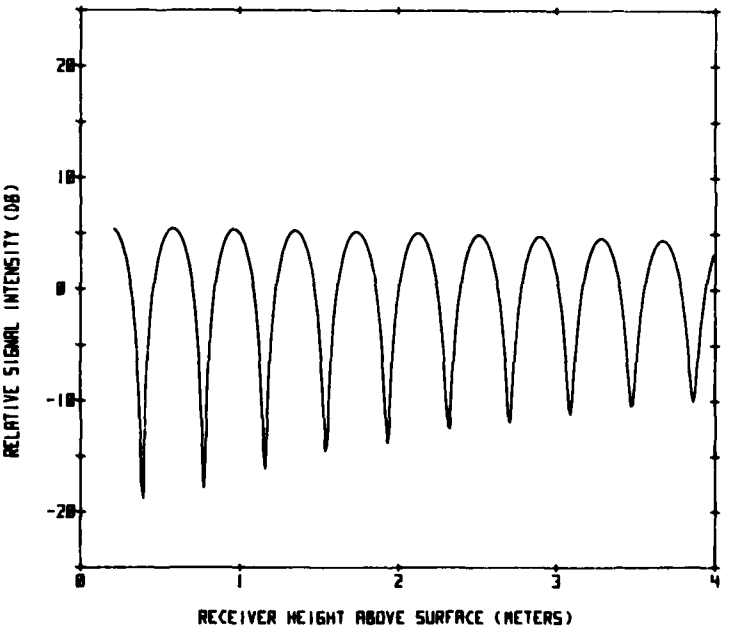

Figure 5. Multipath Signal Over Flat Surface (Frequency 35.1 GHz, Vertical Polarization, $\epsilon_r = 1.12$, Beamwidth 7 deg)

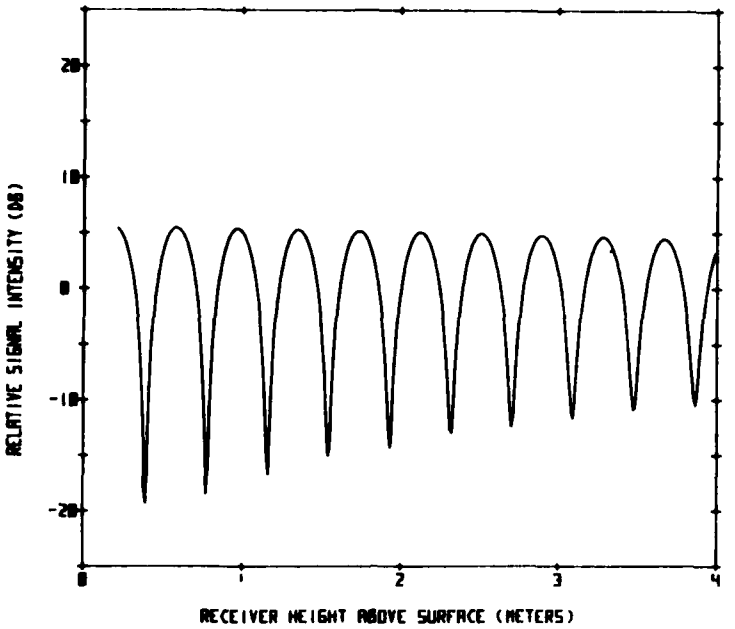

Figure 6. Multipath Signal Over Flat Surface (Frequency 35.1 GHz, Horizontal Polarization, ϵ_r = 1.12, Beamwidth 7 deg)

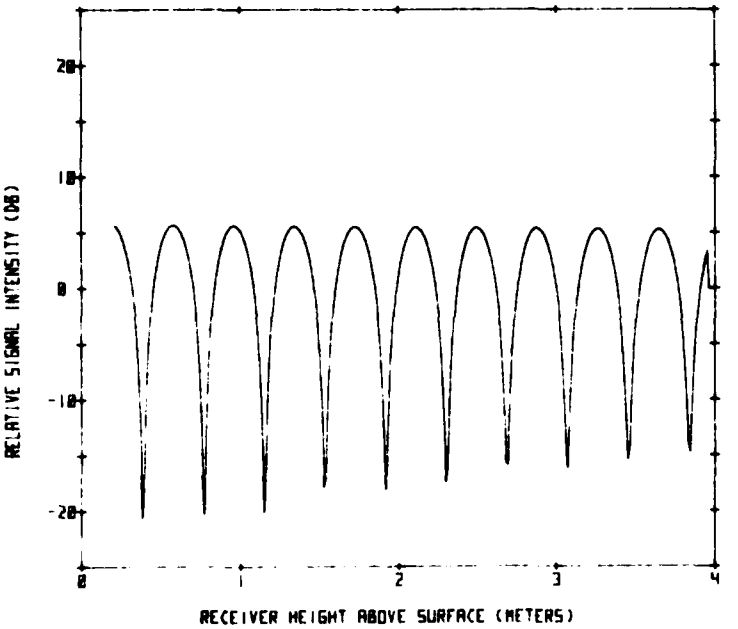

Figure 7. Multipath Signal Over Flat Surface (Frequency 35.1 GHz, Horizontal Polarization, ϵ_r = 1.12, Beamwidth 35 deg)

A significant effect is obtained when both antenna beams are tilted at a constant angle. This is shown in Figure 8. The figure compares with Figure 6 with the exception of a beamtilt of $\delta = -2$ deg, a major portion of the 3 dB-beamwidth. One consequence of the beamtilt are consistently lower peaks, from 0.6 to 1.2 dB. The reduction in antenna gain along the direct path is not compensated for by the increase in gain along the reflected path. Larger changes in dB than this are seen for the minima in the upper portion of the height range. If the reflection coefficient is determined from the ratio of maxima and minima this must be of concern. Conceivably, the antenna beams could be pointed in such a way that for a particular path geometry the losses incurred by the reflected ray upon reflection are compensated for in the direct ray by a reduced antenna gain. Their out-of-phase addition would then lead to perfect cancellation. Neglecting the beam effect this would unrealistically be interpreted as $\rho = 1$. In practice, care is taken to align the antenna in elevation. Besides, the above condition cannot exist over the complete height range and lead to consistently perfect or near-perfect cancellation. Compare again Figures 6 and 8. Increased depth of minima is up to 13.5 dB near the top and around 4 dB near the bottom. Note that a 7 deg-beamwidth in Figure 6 also distorts results against Figure 7, where a 35 deg-beamwidth represents the more ideal, beamwidth-independent case. Comparison of Figures 7 and 8 leads to a better picture. The minima depth in the upper region differs by less than 9 dB and in the lower region by approximately 2.5 dB. During the experimental measurements an alignment error of -2 deg is very unlikely. If the receiving antenna is placed at a local maximum for $h_R \approx h_T$, the angular difference between direct and reflected rays is about 1 deg in our case, with zero phase difference between the signals. If ρ were 1, the greatest sum signal should be obtained with the antennas pointed halfway between the directions of the direct and the reflected ray. With ρ less than 1, this maximum would lie closer to the direction of the direct signal. The maximum angular alignment error with the signal truly peaked would be 0.5 deg in our case. In principle, antenna alignments deviating from zero deg elevation are of no concern, if their angle is known. The effect can then be computed.

Figures 9 and 10 have to be seen in connection with Figure 4. Again all parameters are common to these figures with the exception of frequency. The only difference in the results is the rapidity with which a change in receiver height leads from one signal minimum to the next. At 35.1 GHz 10 minima were counted. At 98.1 GHZ (Figure 9) there are 28 and at 140.1 GHz (Figure 10) there are 40. The ratio of frequency to number of minima at the three frequencies is 3.51, 3.50, and 3.50. The number of lobes is proportional to frequency. More so in Figures 9 and 10 than in Figure 4, the minima do not monotonically decrease with receiver height. This is due to the limited computational accuracy. Most of the calculations were done at 35.1 GHz for this reason, since effects scale with frequency, if they are frequency dependent.

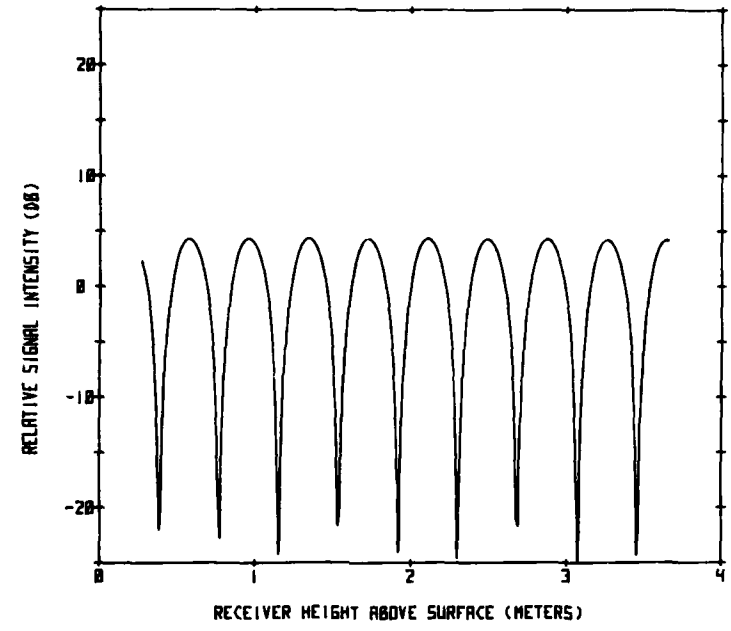

Figure 8. Multipath Signal Over Flat Surface (Frequency 35.1 GHz, Horizontal Polarization, ϵ_r = 1.12, Beamwidth 7 deg, Beamtilt -2 deg)

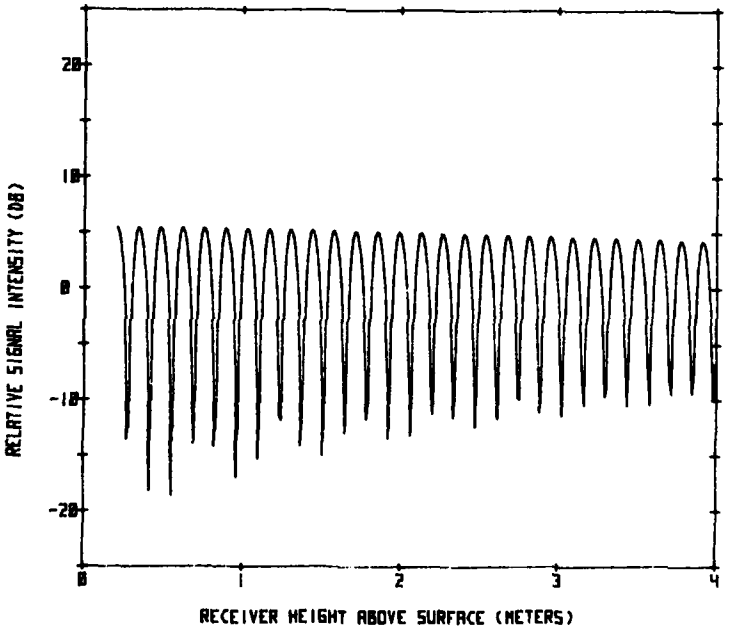

Figure 9. Multipath Signal Over Flat Surface (Frequency 98.1 GHz, Vertical Polarization, ϵ_r = 1.12, Beamwidth 7 deg)

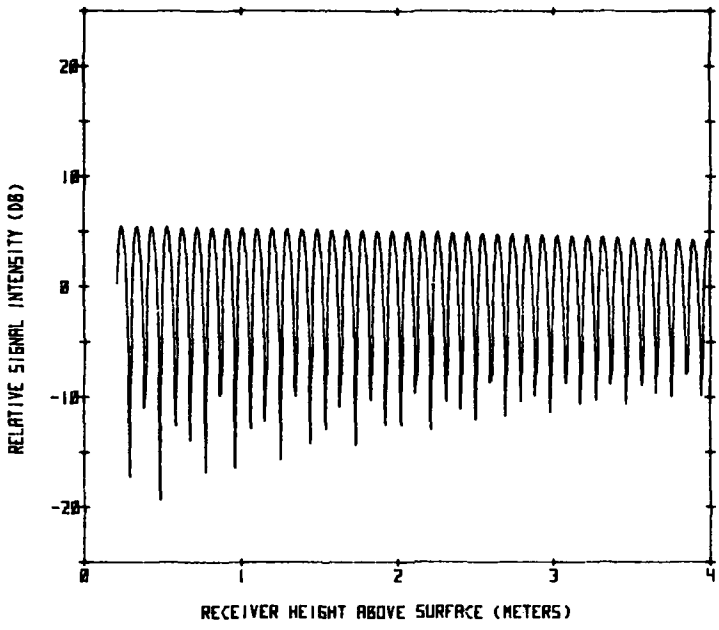

Figure 10. Multipath Signal Over Flat Surface (Frequency 140.1 GHz, Vertical Polarization, $\epsilon_r = 1.12$, Beamwidth 7 deg)

3. PROPAGATION EXPERIMENT

Climatic conditions in the Boston area are such that a sufficient amount of snow can be expected each winter to cover the ground to a depth adequate for millimeter wave propagation measurements. Intervening periods of warmer weather allow the snow to thaw during the day and refreeze during the night, resulting in snow surfaces that are known to be particularly effective in reradiating millimeter waves. This fact along with the necessity of logistic support for the laboratory-type millimeter wave instrumentation prompted us to choose a propagation test site in the vicinity of the RADC laboratory at Hanscom AFB, Massachusetts. Equipment reconfiguration was completed before the end of 1978 with the objective to conduct measurements in the field over the remainder of the season, and specifically through the transition region into spring, when day/night temperature changes are best suited for the formation of metamorphic snow. As it turned out, conditions for multipath measurements during the past winter were not optimal in terms of snow-cover on the ground. While the total amount of snowfall was about normal, most snowstorms ended in a transition to rain, which washed away most of the snowcover.

At no time last winter did the snowcover exceed 10 cm. The equipment performed satisfactorily during the experimental periods. Measurements of snow multipath propagation were conducted on four occasions. Along with measurements over snow, a control measurement was performed on the identical path over dead, matted grass. Figure 11 shows a picture of the general test area with the transmitter in the foreground and the receiving setup in the background.

Figure 11. Experimental Site and Test Setup

3.1 Transmitting and Receiving Equipment

A simplified diagram in Figure 12 presents the basic transmitter and receiver building blocks and a schematic view of the signal paths. A Varian VSA 9010 EW Gunn oscillator at 35.1 GHz and klystron oscillators at 98.1 and 140.1 GHz powered

by separate supplies are on/off modulated by a common squarewave modulator at a 1 kHz-rate. Varian klystrons VC 710C with 75 mW rated output at 98.1 GHz and VRT 2123A with 50 mW rated output at 140.1 GHz are operated at reduced beam voltages of 1500 V for improved frequency stability and extended tube life. Power output could not be measured and is estimated at a few milliwatts. The transmit antennas are standard rectangular gain horns at 35.1 and 98.1 GHz and a scalar feed horn at 140.1 GHz. Beamwidths are listed in Table 2.

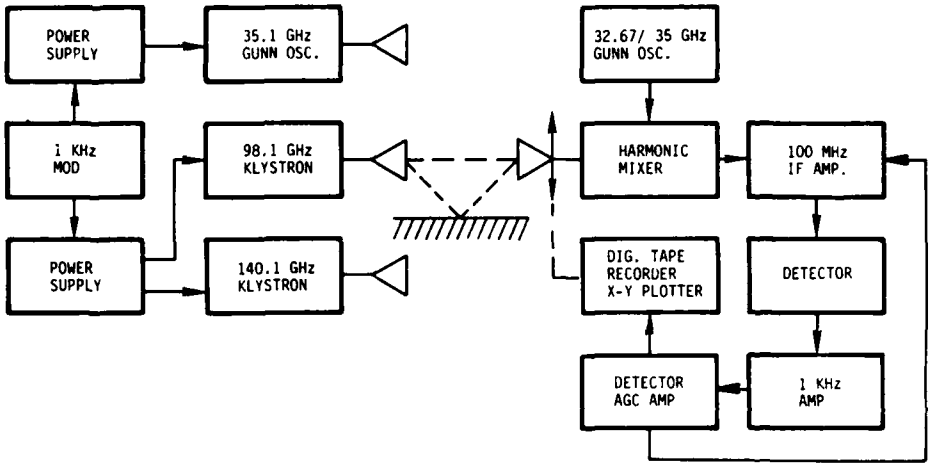

Figure 12 Multipath Equipment Block Diagram

Table 2. E- and H-Plane Beamwidths of Transmitting and Receiving Antennas

Frequency (GHz)	Transmitting Antenna Calc. 3 dB-Beamwidth		Receiving Antenna Calc. 3 dB-Beamwidth	
	β_E (deg)	β_H (deg)	β_E (deg)	β_H (deg)
35.1	9.1	6.8	13.9	11.8
98.1	9.3	7.0	12.1	9.9
140.1	7.2	7.2	8.5	7.0

There is only one common receiver for the three frequencies. The receiver is designed around the TRG A965 single-ended waveguide mixer using a Schottky barrier diode. A Varian mechanically-tuned Gunn oscillator is used as the local oscillator. The specific unit used here (VSA 9010 EW) was found to tune satisfactorily

over a frequency range from 32.67 to 35.0 GHz, substantially exceeding its specified tuning range. Using an intermediate frequency of 100 MHz, the receiver operates with fundamental mixing at 35.1 GHz (L.O. tuned to 35.0 GHz), and with fourth-order harmonic mixing at 140.1 GHz (L.O. tuned to 35.0 GHz). At 98.1 GHz, third-order harmonic mixing is used with the L.O. tuned to 32.67 GHz. An intermediate-frequency bandwidth of 20 MHz was found to be commensurate with the frequency stability of the free-running millimeter wave sources under outdoor temperature changes. Only an occasional retuning was required. The choice of an M-band frequency of 98.1 GHz, which is slightly higher than the center frequency of the atmospheric transmission window, was dictated by the availability of millimeter wave sources and the ease of changing frequencies from one band to another by retuning the L.O. A standard K_a-band gain horn (Table 2) is used to receive the 35.1 GHz signal. A standard M-band gain horn with an M- to K_a-band transition receives at both 98.1 and 140.1 GHz. At the higher frequency the waveguide is oversized. The receiver beam pattern at 140.1 GHz was measured and found to be in agreement with Table 2. The transmitters and the receiver front-end can be rotated by 90 deg for vertical and horizontal polarization. Referring again to the block diagram of Figure 12, the harmonic mixer is followed by a 35 dB IF amplifier, a precision 120 dB step attenuator (HP 355B), two cascaded balanced mixers (Z-MATCH DBM-100B) connected as electronically controlled variable attenuators with a range in excess of 70 dB for automatic gain control (AGC), and another 35 dB amplifier. After detection, the 1 kHz-squarewave-modulated signal is amplified in a HP 415E Standing Wave Indicator (bandwidth 15 Hz) and rectified. The output signal drives the AGC amplifier, whose gain curve was adjusted for a near-logarithmic receiver response over a 50 dB input signal range. The rectified 1 kHz signal also drives the Y-axis of a Moseley X-Y recorder. The X-axis signal is a potentiometer-derived dc voltage proportional to the receiver height on the vertical positioner. The same signals are also stored in digital form on magnetic tape for later processing.

The time constant of the receiver is essentially determined by the mechanical time constant of the X-Y recorder. The recording speed, that is, the speed of vertical receiver motion was empirically set so that the recording system could trace the actual signal excursions. The boom of the sled holding the transmitters in Figure 11 does not serve the purpose that it was originally designed for in the backscatter measurement program, where a snow sample was rotated in a basket at the boom midpoint. Here we use the structure only to support the transmitting antennas at a height of 2 m above the surface.

The vertical positioner consists of a 5.1 by 5.1 cm square aluminum shaft of 4-m height, held upright by a tripod on the ground, each leg of wood and 1.80-m long. A small carriage rides on eight ball bearings directly on the square aluminum

shaft. A sketch of it can be seen in Figure 1. The carriage is suspended from an endless gear drive belt, operated by a motor-driven gear belt pulley on the bottom of the shaft. The belt itself operates a ten-turn potentiometer from another gear belt pulley at the top of the shaft. The position voltage is derived from this potentiometer. The carriage has a small platform on which the receiver front-end is mounted. The remaining components of the receiving equipment are mounted on the laboratory cart visible to the left of the vertical positioner in Figure 11.

3.2 Propagation Test Site

The terrain selected for multipath measurements is a relatively plane field, on which the grass is cut during the summer. There is no vegetation other than grass and weeds in the vicinity of the propagation path. Again, Figure 11 gives an idea of the general appearance of the test site. The lack of contrast in the snow makes the area look slightly smoother than it is in reality. Within 20 m to the right of the transmitter, parallel with the road in the background, is a three-story laboratory building extending over a part of the length of the field. Otherwise, the field is in a natural condition, surrounded by trees. The area is approximately 100 by 200 m in size. A terrain profile was determined along the preferred propagation path, which is displayed in Figure 13.

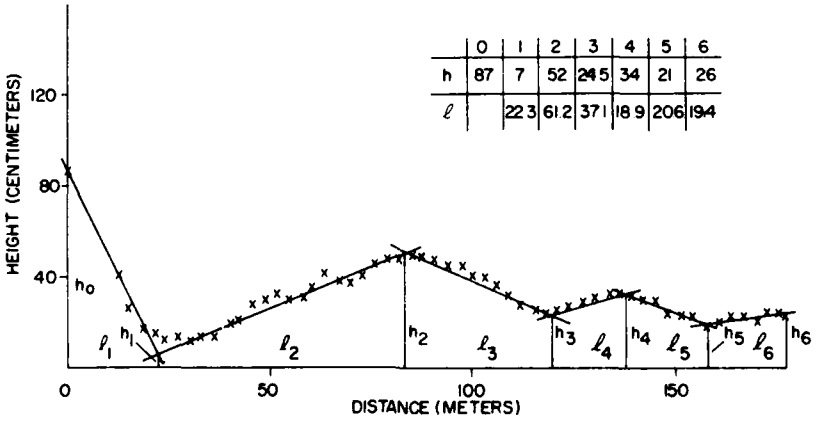

Figure 13. Terrain Profile Measured on Snow Path

Relative terrain height was measured at fixed intervals, using a telescope with crosshairs and a meter stick. Measurement accuracy is ± 1 cm or better. Heights measured, however, were local heights with no consideration given to averaging over fine structure. Also, there may be a general slope to the terrain, not detected

by the simple measurement technique. This is of little concern, since it does not affect the millimeter wave measurements. As shown in Figure 13, the actual heights were approximated by six straight-line segments, which represent an empirical best fit to the actual heights. Values for h_n, ℓ_n were derived for the straight-line segments. The heights are referenced to an arbitrary level. The calculated values in the table associated with Figure 13 show h_0 through h_6 in centimeters and ℓ_1 through ℓ_6 in meters. No measurements were made of the snow profile superimposed over the terrain profile, in order not to destroy the snow surface by footprints. It is assumed that the terrain profile represents the snow profile with reasonable accuracy. Snow height measurements and other snow ground truth measurements were conducted in the vicinity of the propagation path.

3.3 Ground Truth Measurements

The backscatter measurements obtained through the more normal winter season 1977/78 were complemented by a comprehensive set of ground truth measurements, performed near the scatterometer site. Snow properties checked on a daily basis included depth, density, temperature, stratigraphy, microstructure, surface characteristics, and free-water content. The majority of the properties were determined using equipment supplied in the Snow Observation Kit designed by the US Army Cold Regions Research and Engineering Laboratory, Hanover, New Hampshire. The preliminary nature of our multipath measurements is also due to a somewhat limited set of ground truth measurements. It is assumed that all propagation data were obtained over snow in the frozen or dry state, though there were no simultaneous calorimetric analyses performed. Measurements that were made include air temperature, snow temperature, density, hardness, particle size, and general observations about the reflecting surface. A weather diary was kept to characterize local meteorological conditions that might have a bearing on the results. This diary was kept on most days, regardless if propagation measurements were made or not. Multipath measurements to be reported here were performed on four days in February.

(1) On 2 February, a sunny and windy day, snow of no more than 3 cm depth was on the ground, with a limited number of blades from the underlying dry grass penetrating the snow surface. The maximum temperature for the day was -3° C. The wind uncovered some spots from snow during the day. Light snowfall had occurred on the previous two days, which appeared to be wet on the first day. On 2 February the movement of snow due to wind was strong enough to cover footprints in a few hours.

(2) The day of 7 February was sunny early and cloudy later on. The temperature remained at around -6° C, but the humidity increased to produce a damp, cold sensation. All snow on the ground had disappeared during the 2 to 7 February period. Snow began falling after the end of the multipath measurements and continued falling through the night.

(3) On 8 February the temperature was still at -6° C. Snow stopped falling around 9 a.m. after 5 to 8 cm had accumulated on the ground. This snow was very light and fluffy. A density of 0.08 g/cm^3 was determined. Crystal size was approximately 2 to 3 mm. During the propagation tests it was calm and sunny with air and snow temperatures in the shade of -4° C.

(4) The last measurements were made on 28 February. Two days earlier granular, wet hydrometeors fell during most of the day, accumulating to a height of 8 cm on the ground. We elect to call this form of precipitation sleet, following the definition of Petterssen.[5] It was clearly different from wet snow, which has a much softer consistency, and it was not freezing rain, as was experienced during the latter part of that day. Temperatures hovered around the freezing point, and the material deposited on the ground essentially remained as it had fallen. On 27 February, day time temperatures stayed at -2° C under a cloudy sky and light snow began to fall. These conditions made it possible for the sleet on the ground to freeze over. On 28 February, a sunny day, a snow temperature of 0° C and an air temperature of +1° C were measured. The highest air temperature on this day eventually reached +10° C. The frozen sleet had a very hard surface capable of supporting a person walking on it. Hardness measuremes were offscale. (greater than 50 kg/cm^2). A density of 0.47 g/cm^3 was determined. Visual inspection revealed mostly spherical particles of 1 to 2 mm diameter, with some as large as 3 mm.

3.4 Millimeter Wave Measurements

In order to conduct multipath measurements on a day that appeared suitable, the equipment had to be moved into the field. After assembly and direction alignment, both by physical sighting and signal peaking (the latter at a receiver height of about 2 m). a data run was made. The receiver was generally lowered from maximum height during this run, which resulted in a slightly more uniform receiver velocity over the whole height range. After completion of the run, the receiver was elevated to the point of highest received signal, generally in the lower third of the height range. At this point calibration levels were marked on the recording and on magnetic tape, corresponding to 10 dB steps below the maximum received signal.

5. Petterssen, S. (1958) Introduction to Meteorology, McGraw-Hill, New York, New York.

This calibration allows us to determine local peak-to-valley differences of constructive and destructive interference. Measurements were restricted to calm or moderate-wind periods, although a sway of several centimeters at the top of the vertical positioner appeared to have little effect on the signal phasing. Since the receiver has a response somewhat different from a truly logarithmic one, measured curves had to be replotted later to obtain a linear dB scale. Tests conducted at the three frequencies were somewhat arbitrary in sequence, and mostly done in a way that a minimum of equipment reconfiguration was necessary. Transmitters were switched on or off as required and used after a warmup time of 5 min each. They could not be operated continuously because of the shared power supply and the danger of cross-reception. Note that the receiver is simultaneously tuned to 35.1 and 140.1 GHz. Changing frequencies at the receiver end required a change of antennas between 35.1 and 140.1 GHz, or a retuning of the local oscillator between 98.1 and 140.1 GHz. No further changes were made to the receiver such as retuning the mixer, which might have resulted in a somewhat higher sensitivity. Over the distance of 179.5 m, dynamic ranges of 50, 40, and 30 dB were achieved at 35.1, 98.1, and 140.1 GHz, respectively. This was satisfactory over the terrain and the types of snowcover of last winter. The time required for a data run including frequency change is of the order of 30 minutes.

4. ANALYSIS OF EXPERIMENTAL DATA

It has been shown under somewhat idealized conditions that the phase interference technique serves to determine the snow reflection coefficient. If the terrain is not flat, nearly uniform lobing as seen in Figures 4 through 10 can no longer be expected. Before analyzing the measured data, we will model multipath propagation over the actual terrain profile, to determine the effects of the local terrain height and slope. The model considers only major terrain features and their contribution to a specular reflection process. At low angles of incidence and reflection there is the possibility of terrain interaction at places other than the reflection point. Shielding or multiple reflections are not considered in the context of the model.

4.1 Model Calculations for Actual Terrain

The computer model described in Section 2.2 was used to simulate multipath signals over the terrain profile of Figure 13. In the modeling of propagation over flat terrain in Section 2.2, $\epsilon_r = 1.12$ for light snow and $\epsilon_r = 1.92$ for metamorphic snow was used. These numbers were derived from the ground truth measurements

on 8 and 28 February [cases (3) and (4) of Section 3.3]. They follow from Eq. (20), after converting the densities measured into fractional volumes filled by solid ice, assuming that the ice does not contain free water. The next series of graphs are all computed for $\epsilon_r = 1.12$. There is no major change for higher ϵ_r, as was seen in Figures 4 and 5. For the same reason all graphs are for horizontal polarization.

It has been found that the received signal is dependent on both the straight segments and on the circular transition regions. A straight terrain segment generally adds to the received signal only over a limited height range. Its inclination is constant and the change in height at which a multipath signal intercepts the receiver ordinate is small per unit-length change of the reflection point along the surface. In contrast, as the reflection point moves along a circular region, the change in inclination per unit-length change along the surface has a stronger effect on where the reflected ray passes through the receiver ordinate than the change along the path itself. A wider range of heights is covered by the reflected ray, when it passes through the circular region. The choice of the length of the circular region, which directly affects the rate of change of the inclination, has a considerable effect on the appearance of the received height-gain pattern. At any given height on the receiver ordinate, only one or two signals reflected from straight segments may contribute to the sum signal. This is because the reflection point distance from the transmitter, its height and local inclination have to agree. In the circular region, this agreement is reached in more cases, because the local inclination covers a large, contiguous range of values, including one where the reflection conditions for the particular receiver height is met. Actual measurements over snow suggest that a limited number of reflected signals plus the direct signal compose the received signal at any height. In order to simulate a similar signal structure, the number of circular transition regions and hence linear segments must be kept low. The model is correct in a qualitative way, based on relatively simple terrain features. It cannot be expected to yield one-to-one correspondence between model and measured height-gain patterns, since this would require much greater precision in describing the path profile. In Figure 14 we assume a circular transition from one linear segment to the next to begin 5 m from the end of each segment. Typical radii of hundreds of meters can be expected for the terrain profile of Figure 13. The 0 dB level in Figure 14 corresponds to the direct signal of unity amplitude. An in-phase addition of a reflected signal of equal amplitude results in a sum signal of 6 dB. Three reflected signals and the direct signal add up to 12 dB, if they are of unity amplitude and optimally phased, and so on. This optimal phasing will not likely occur with an increasing number of reflected signals, and hence the sum signal will not reach its maximum height. In the negative direction, extinction between the direct signal and one reflected signal will not exceed a level given by the magnitude of ρ, even under perfect out-of-phase addition. This

assumes that the antenna gains are comparable. With one or more reflected signals added, there is a chance of a more complete extinction of the sum signal. The general trend observed in Figure 14 is typical of modeled and measured patterns. At the greater receiver height and the reflection taking place more toward the transmitter, there is only a single reflected signal interacting with the direct signal. This is apparent for heights above 2 m in Figure 14, which has a similar appearance in this range to Figure 6. The maximum amplitude is close to 6 dB. Below 2 m height, at least three phasors interact, because the sum vector reaches a level of 10 dB. In principle, another reflected signal could be present, with the phasing never reaching an optimum so that the sum signal could approach 12 dB. In the same region, at 0.6 m height, cancellation stronger than in Figure 6 is observed (23.4 dB vs 19.4 dB). This requires the superposition of more than two components. Some raggedness in the curve must be attributed to the imperfections of the computer simulation. In Figure 15 the circular transition region is reduced in length and starts at a point 1 m from the segment end. It is apparent by comparison with the previous figure that the curve shows several major changes. This must not be interpreted as a failure of the model. Again, the model and the precision of its input parameters are only adequate to deliver a qualitative picture, and to point out qualitative features of the multipath propagation phenomenon. It cannot produce deterministic correspondence. Close inspection of Figure 15 reveals approximately the same positions for most of the minima, where they still exist. At 2 m height, the minimum has been replaced by a minor peak. At 1.5 m and 1.1 m height the minima have increased in depth. At around 0.6 to 0.8 m height, the deep minimum has changed to two minor maxima. This is not surprising on consideration of the different curvature and heights within the transition region. In Figures 16 and 17 the same equipment factors as in Figures 7 and 8 are tested. A much wider beam of 35 deg as in Figure 16 has the only effect of widening the peak-to-valley range in most cases by about 5 dB. Likewise, a negative beamtilt of 2 deg in Figure 17 leads to systematically greater null depths at greater heights of 7 to 9 dB relative to Figure 16. Below 2 m receiver height the null depth is even less than in the 35 deg case by 2 to 7 dB. This occurs despite the fact that the antenna beams favor the direction of reflection over the direct path. This is apparent by a sum signal about 1 dB lower at all heights in Figure 17. In general we conclude that equipment factors do not systematically affect our results. Note also that most experimental antenna beamwidths (Table 2) exceed the 7 deg value assumed in the calculation.

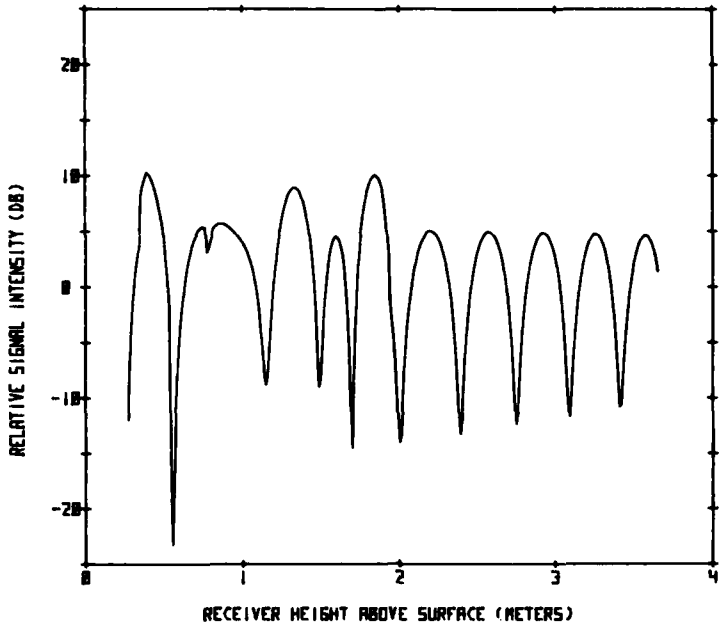

Figure 14. Multipath Signal Over Six-Segment Profile (Frequency 35.1 GHz, Horizontal Polarization, ϵ_r = 1.12, Beamwidth 7 deg, Circular Region 5 m)

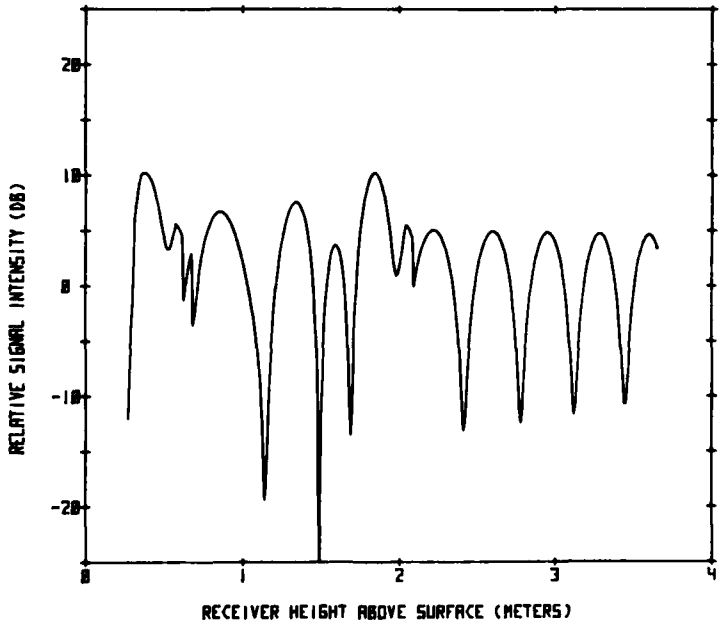

Figure 15. Multipath Signal Over Six-Segment Profile (Frequency 35.1 GHz, Horizontal Polarization, ϵ_r = 1.12, Beamwidth 7 deg, Circular Region 1 m)

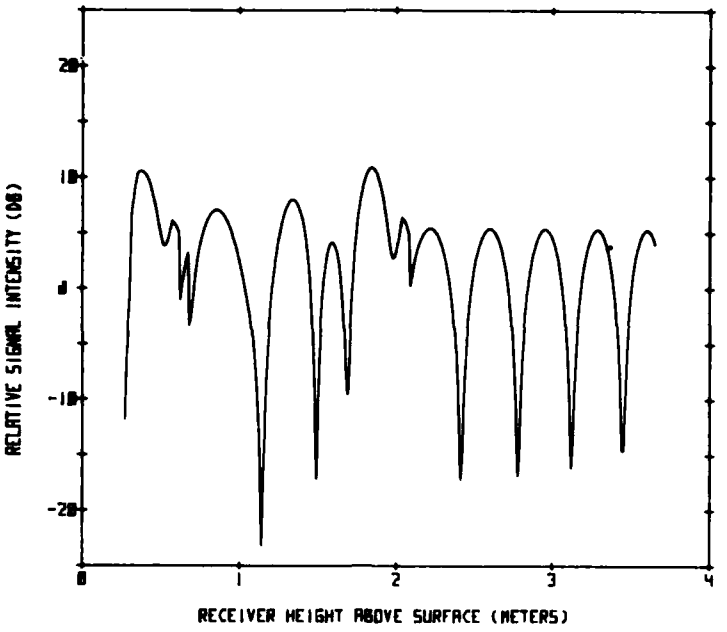

Figure 16. Multipath Signal Over Six-Segment Profile (Frequency 35.1 GHz, Horizontal Polarization, ϵ_r = 1.12, Beamwidth 35 deg)

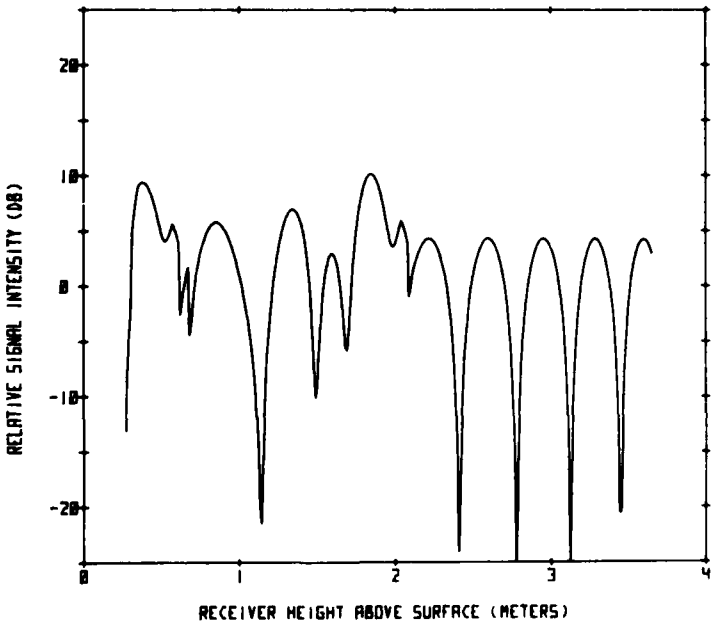

Figure 17. Multipath Signal Over Six-Segment Profile (Frequency 35.1 GHz, Horizontal Polarization, ϵ_r = 1.12, Beamwidth 7 deg, Beamtilt -2 deg)

4.2 Multipath Propagation Over Matted Grass

A series of tests was conducted on 7 February [Section 3.3, case (2)] over dead grass for comparison with the snow measurements. The grass had been pressed to the ground by previous layers of snow and presented a relatively flat surface. This suggests that the electromagnetic wave, before and after reflection, penetrates little vegetation, which would cause attenuation and reduce the reflection coefficient. Figures 18 and 19 show the multipath performance of the 35 GHz system for horizontal and vertical polarization. As expected, both curves resemble each other closely at the low grazing angles involved. The majority of the maxima and minima in the earlier one exceed those of the latter one only slightly. The difference is predicted by the respective magnitudes of the reflection coefficient, with some effects perhaps due to antenna alignment.

The 0 dB level in the experimental curves was set at the highest sum signal received. In contrast, 0 dB in the model curves was placed at the height of the direct signal only. This simplifies the procedures and is of no importance, since we are concerned with signal differences.

A predominant feature in Figures 18 and 19 is the low minimum at about 1 m height. Following earlier reasoning we conclude that this is the superposition of the direct signal and at least two reflected components. If we assume that only a single reflected signal interacts with the direct signal in the height range from 2.30 m to 3.30 m, then $\Delta V = 10.3$ dB. Using Eq. (23) to convert ΔV to the magnitude of the reflection coefficient over matted grass, we obtain $\rho = 0.53$.

Figure 20 shows the same conditions for 98 GHz. An amplitude range for two-signal interaction, $\Delta V = 4.7$ dB is estimated, which converts to $\rho = 0.26$. In Figure 20 and in Figure 21, the corresponding 140 GHz graph, it becomes increasingly more difficult to establish a region of two-signal interaction. This demonstrates the limit of the phase interference technique in establishing the magnitude of the reflection coefficient. We estimate from Figure 21 that $\Delta V = 3.6$ dB and $\rho = 0.20$. Wallace[6] has measured the multipath performance of a 140 GHz monopulse antenna over weeds, grass and asphalt. His equipment to determine height-gain patterns is similar to ours. Antenna heights are comparable but the range is only 100 m. He concludes that the magnitude of ρ for vegetative ground cover is less or equal to 0.1. This most likely includes the effect of substantial attenuation from growing grass and weeds, where the grass was mowed and the weeds reached a height of 1 m. Maximum signal excursions observed over the test range covered with dead grass are 25.6 dB, 16.7 dB, and 10.0 dB at 35, 98, and 140 GHz, respectively.

---

6. Wallace, H. B. (1978) 140-GHz Capture Antenna Multipath Experiment, Memorandum Rep. ARBRL-MR-02855, Ballistic Res. Lab., Aberdeen Proving Ground, MD.

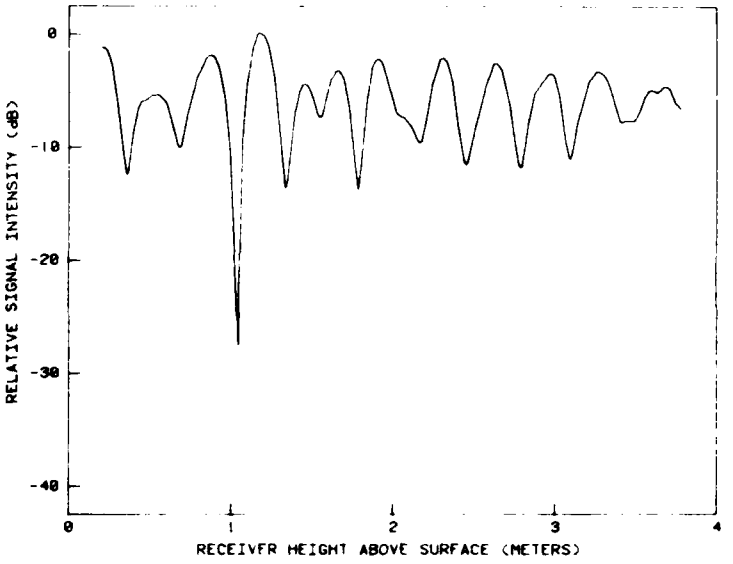

Figure 18. Multipath Signal Over Matted Grass (Frequency 35.1 GHz, Horizontal Polarization)

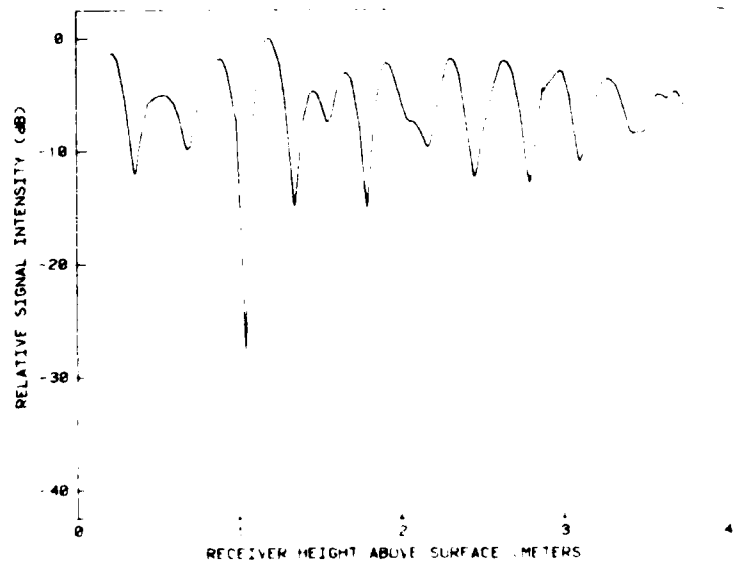

Figure 19. Multipath Signal Over Matted Grass, (Frequency 35.1 GHz, Vertical Polarization)

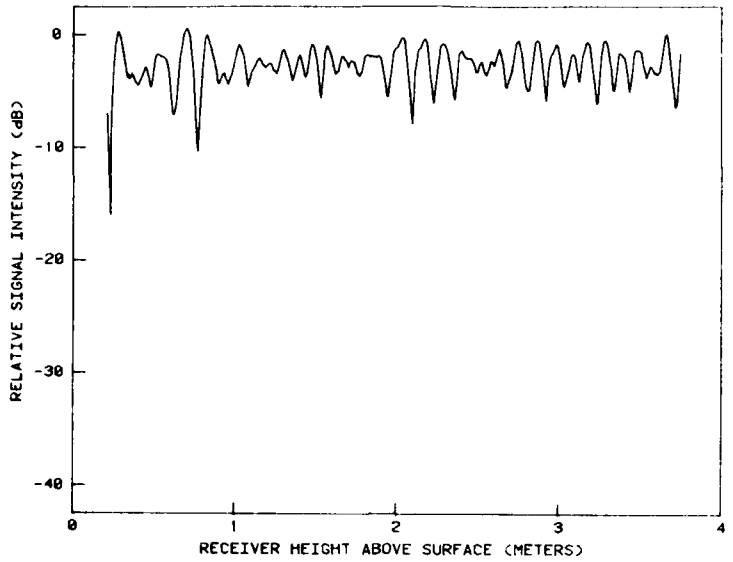

Figure 20. Multipath Signal Over Matted Grass (Frequency 98.1 GHz, Vertical Polarization)

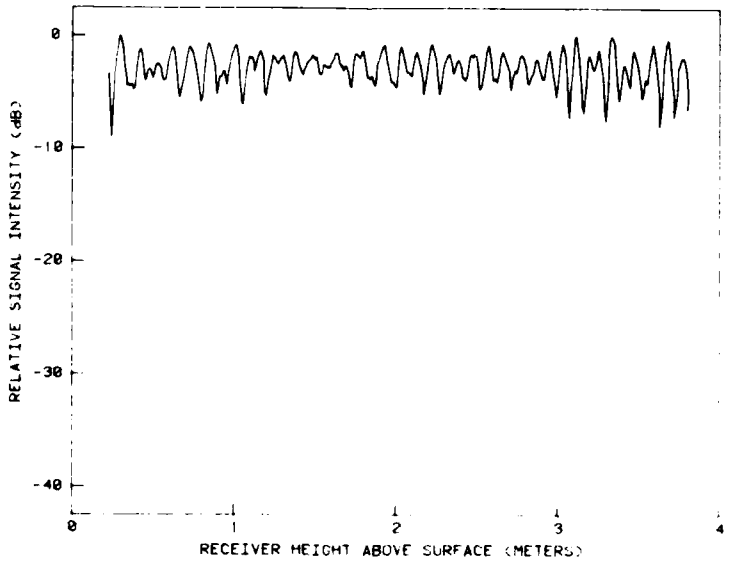

Figure 21. Multipath Signal Over Matted Grass (Frequency 140.1 GHz, Vertical Polarization)

4.3 Multipath Propagation Over Snow

The only series of data at all three frequencies over snow, obtained on the same day, is shown in Figures 22, 23, and 24. The meteorological conditions prevailing on 8 February are described in Section 3.3, case (3). Following the same procedures as before, we establish values $\Delta V = 13.9$ dB, $\rho = 0.66$, maximum excursion 25.8 dB at 35 GHz, $\Delta V = 8.9$ dB, $\rho = 0.47$, maximum excursion 27.8 dB at 98 GHz, and $\Delta V = 6.1$ dB, $\rho = 0.34$, maximum excursion 20.6 dB at 140 GHz. The snow data best suited for comparison with our measurements have been produced by Cornwall et al,[7] at a frequency of 9.1 GHz. Their range of grazing angles varied between 1.5 and 5 deg over a path of 2052 m, also in Massachusetts. The equipment was capable of distinguishing between the direct and the reflected signal contributions on the basis of arrival time. Figure 4.2-16(a) of their report indicates a reflected power measured 9 dB below the direct power at a transmitter elevation of 3 deg, which we can roughly take as the grazing angle on flat snow-covered terrain. The reflected signal is attributed at this angle to equally strong specular and diffuse components. The specular component increases at a rate of 6 dB per degree with the grazing angle decreasing from 4 to 3 degrees. It is difficult to extrapolate to our angular range, where certainly specular reflection dominates. No data were reported over snow at the 1.5-deg grazing angle, If the 3-deg data were originated from specular reflection, we would calculate $\rho = 0.35$, increasing toward lower grazing angles.

On 2 February, measurements were only performed at 35 GHz. These were the initial measurements using the modified equipment, and were intended as a test. The snow cover was so thin, it was assumed that measured multipath interference was mostly coming from the ground with negligible influence from the snow. In reality this snow cover composed of a thin layer of granular structure resulted in the strongest multipath interference seen so far at 35 GHz. The effect of the thin snow layer in Figure 25 is illustrated, when comparing this figure with Figure 19. The height region from 2.3 to 3.3 m is evaluated for $\Delta V = 21.9$ dB and $\rho = 0.85$. The greatest signal excursion is 27.5 dB. It is interesting to note the similarities of this figure and Figure 16, a simulation under similar conditions. In the upper third of the height range we find two-signal phasing. Below it, minor peaks from higher number interactions occur with a similar range of amplitudes. The deepest cancellation takes place around a height of 1 m. The parameters inferred from the model curve are $\Delta V = 22.2$ dB and $\rho = 0.86$. The greatest excursion is 34.2 dB. At around 4 m receiver height the computer uses $\rho = 0.82$ to compute the model curve. The remaining Figures 26 and 27 may be considered in connection with

7. Cornwall, P.E., Green, A.H., and Armstrong, D.G. (1977) Multipath Measurements Phase III, Final Tech. Rep. ER 77-4121, ARPA Order No. 2731.

Figure 25, in the sense that they constitute a set of data for all three frequencies over granular snow. It must be realized that Figures 26 and 27 were obtained on 28 February under vastly different meteorological conditions, as listed under Section 3.3, case (4). The increase in number of deep cancellations is clearly visible in all three figures in this set. In Figure 26 we estimate $\Delta V = 18.1$ dB, $\rho = 0.78$, and the maximum signal excursion at 25.6 dB for the 98 GHz case. In Figure 27 we estimate $\Delta V = 15.3$ dB, $\rho = 0.71$, and the maximum signal excursion at 27.5 dB. Wallace[6] reports an approximate value at 140 GHz of $\rho = 0.5$ over asphalt. All ρ values were obtained for grazing angles near 2 degrees. In Figures 4, 9, and 10, the model calculations yielded 10, 28, and 40 lobes at 35, 98, and 140 GHz, respectively. A count of lobes in Figures 25 through 27 result in 12, 33, and 50. This count is somewhat subjective, depending on what size lobe constitutes a major one. It must, however, be emphasized that the relatively close resemblance between the counts (theoretical specular model vs experimental data) was the primary reason to treat our multipath propagation phenomenon as specular.

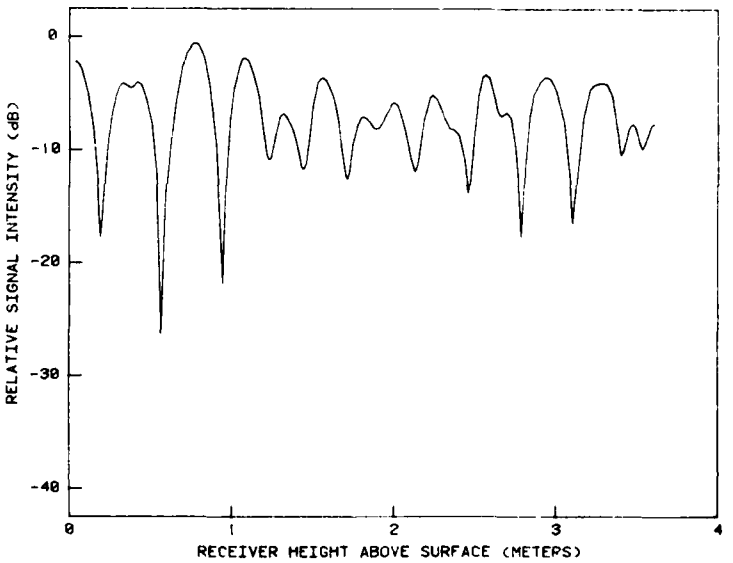

Figure 22. Multipath Signal Over Freshly Fallen Snow (Frequency 35.1 GHz, Vertical Polarization)

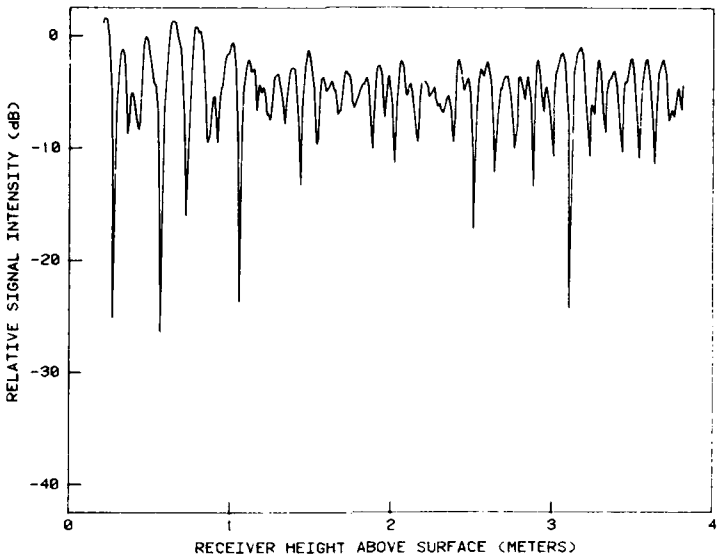

Figure 23. Multipath Signal Over Freshly Fallen Snow (Frequency 98.1 GHz, Vertical Polarization)

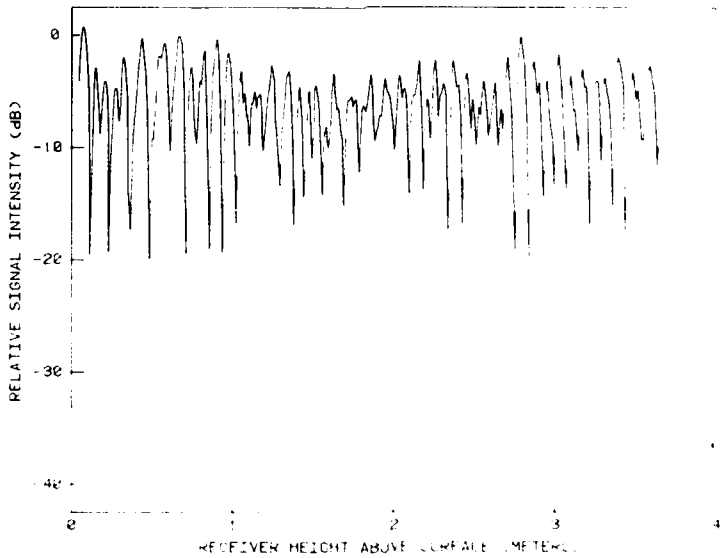

Figure 24. Multipath Signal Over Freshly Fallen Snow (Frequency 140.1 GHz, Vertical Polarization)

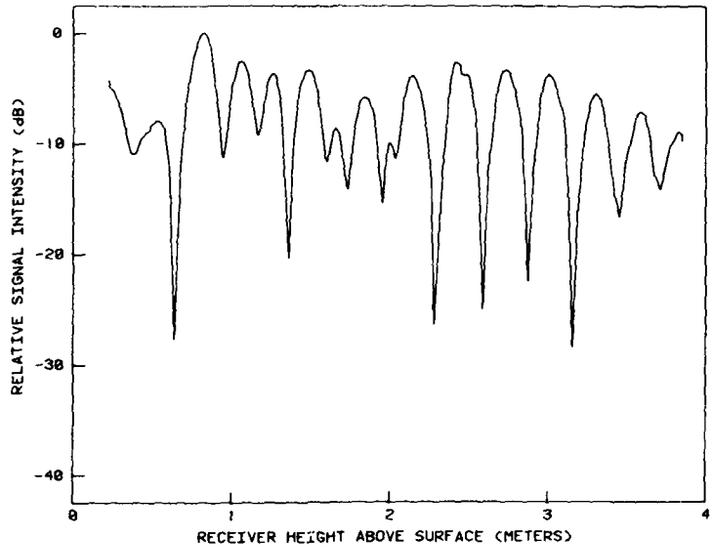

Figure 25. Multipath Signal Over Thin Layer of Old Snow (Frequency 35.1 GHz, Vertical Polarization)

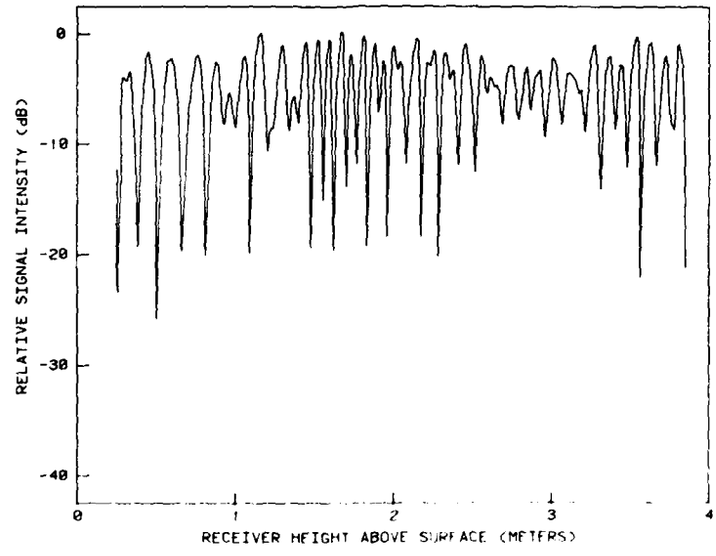

Figure 26. Multipath Signal Over Frozen Sleet (Frequency 98.1 GHz, Vertical Polarization)

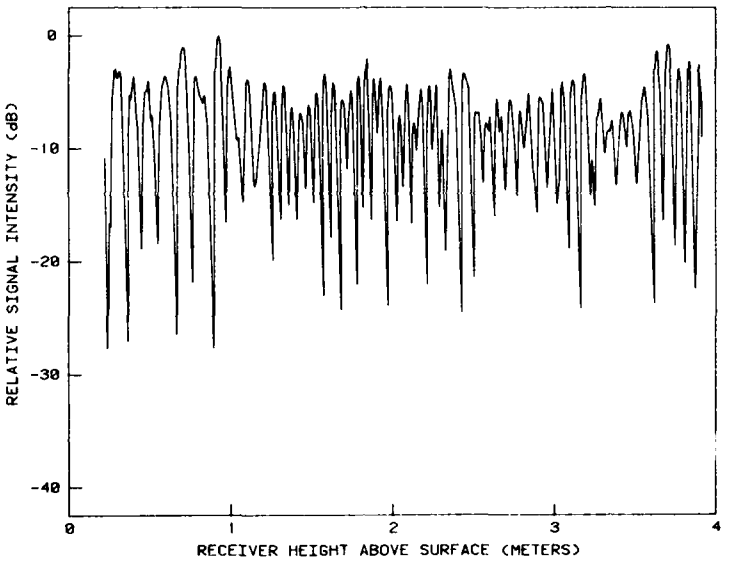

Figure 27. Multipath Signal Over Frozen Sleet (Frequency 140.1 GHz, Vertical Polarization)

5. CONCLUSIONS

A number of preliminary measurements of multipath propagation over terrain covered with dead grass or snow have been presented. At the range of grazing angles of 0.5 to 2 deg and over a relatively flat surface, the sum signal received appears to be composed of a limited number of phasors, typical of specular reflections from one or a few sections of the terrain along the propagation path. A model was composed, based on the relevant parameters of the experimental setup including major features of the terrain, in order to study the effects of several of these parameters, to simulate multipath affected height-gain patterns for comparison with measured patterns, and to establish a method for deriving the magnitude of the reflection coefficient. The model calculations at 35 GHz show good agreement with the measurements, in terms of such features as number of lobes, cancellation depths, number of phasors involved. The general appearance is similar in a qualitative way, considering the fact that the surface model was based on terrain heights and not snow heights, which were not measured. At 98 and 140 GHz, terrain roughness becomes more of a factor over the same terrain and the same range of grazing angles. However, the number of measured lobes does not increase significantly over that expected for two-signal interaction for the given path geometries

and flat terrain. Specifically, reflection coefficients range from 0.53 to 0.20 over matted grass, from 0.66 to 0.34 over freshly fallen snow, and from 0.85 to 0.71 over old snow. The higher numbers correspond to 35 GHz, the lower numbers correspond to 140 GHz. The specific values for ρ must be used with caution. Neither have sufficient data been accumulated to firmly establish these numbers, nor does the measurement technique lend itself to a simple derivation of ρ. The measurements do give an indication of the range of constructive and destructive phase interference that one can expect at the particular frequency and angular range over various types of ground cover, if the antenna beam cannot discriminate against surface reflections.

Further measurements, planned for the winter 1979/80, will be conducted with a more complete ground truth measurement program. In addition, shorter and flatter paths will be selected to establish accurate numbers for ρ at the higher frequencies. On the other hand, attempts will be made to extend the measurements over longer ranges and varied terrain to better simulate operational conditions.

References

1. Hayes, D.T., Lammers, U.H.W., and Marr, R.A. (1980) Scattering From Snow Backgrounds at 35, 98, and 140 GHz, RADC Tech Rep. (to be published).
2. Barton, D.K. (1977) Reflection coefficients of snow, Appendix III in Multipath Measurements Phase III, Final Tech. Rep. ER 77-4121, ARPA Order No. 2731.
3. Cumming, W.A. (1952) The dielectric properties of ice and snow at 3.2 centimeters, J. Appl. Phys. 23(No. 7):768-773.
4. Ray, P.S. (1972) Broadband complex refractive indices of ice and water, Appl. Optics 11(No. 8):1836-1844.
5. Petterssen, S. (1958) Introduction to Meteorology, McGraw-Hill, New York, Chapter 3.
6. Wallace, H.B. (1978) 140-GHz Capture Antenna Multipath Experiment, Memorandum Rep. ARBRL-MR-02855, Ballistic Res. Lab., Aberdeen Proving Ground, MD.
7. Cornwall, P.E., Green, A.H., and Armstrong, D.G. (1980) Multipath Measurements Phase III, Final Tech. Rep. ER 77-4121, ARPA Order No. 2731.

MISSION
of
Rome Air Development Center

RADC plans and executes research, development, test and selected acquisition programs in support of Command, Control Communications and Intelligence (C^3I) activities. Technical and engineering support within areas of technical competence is provided to ESD Program Offices (POs) and other ESD elements. The principal technical mission areas are communications, electromagnetic guidance and control, surveillance of ground and aerospace objects, intelligence data collection and handling, information system technology, ionospheric propagation, solid state sciences, microwave physics and electronic reliability, maintainability and compatibility.

Printed by
United States Air Force
Hanscom AFB, Mass. 01731

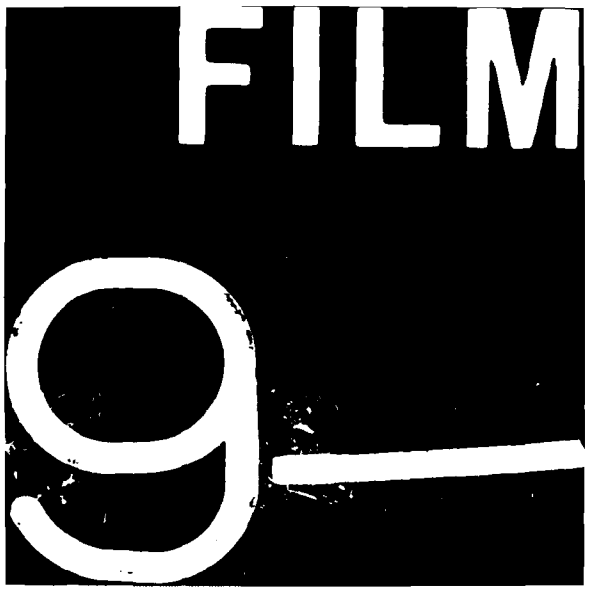
FILM
9-1